System Application and Performance

The electronically scanned antenna array is utilized in an airborne microwave radiometer imaging system. As shown in the block diagram of Fig. 8, this system consists of four basic parts: 1) the antenna with its associated drive and control network, 2) the Dicke switching network, including the calibration and control subsystem, 3) the receiver, and 4) the data processing and display system.

Electromagnetic energy emitted from the surface of the earth is received by the array antenna. The magnitude of this energy is proportional to the radiometric temperature observed. By comparing this energy with that emitted by a known calibration standard, normally a hot and/or cold reference load, it is possible to determine the radiometric temperature of the body seen by the antenna. A two-dimensional map of the radiometric temperature of the earth is therefore generated when the antenna beam is scanned as the vehicle moves.

The radiometer receiver is a solid-state superheterodyne double sideband receiver. Included in this receiver are a balanced mixer, solid-state local oscillator and multiplier, synchronously tuned IF amplifier, square law detector, preamplifier, and synchronous detector. The overall noise figure of the receiver ranges between 6.0 and 7.0 dB. The measurement accuracy and sensitivity of the receiver are 2.0°K and 0.7°K, respectively.

Data processing is performed by a digital data acquistion system which produces a computer-compatible tape output. A real-time grey level display, an analog readout, and a digital printout are also generated simultaneously. The tape output can be processed to give either a grey level display or a color presentation, the latter offering almost a sixfold increase in display resolution.

Scanning of the antenna beam is accomplished in an incremental manner. A total of 39 steps are required to move the beam through the 100° angular range. Each step corresponds to a half-power beamwidth interval. The time required for a complete scan is adjustable to one or two seconds. This includes the time required to reposition the beam to each of the 39 positions and the dwell, or integration, time at each position.

Typical of the data that have been obtained with this system by the NASA Goddard Space Flight Center are those shown in Fig. 9. This radiometric map of the Southern California coastal area was obtained from an altitude of 37 000 feet. The black to white span on the grey level scale represents a temperature range of 228°K to 290°K.

Conclusions

A 19.35-GHz electronically scanned two-dimensional phased array has been described in detail. It has been shown that this configuration is compatible with the overall airborne microwave radiometer system requirements. The phased array described here has a high beam efficiency, can be scanned rapidly, is volumetrically compact and light in weight, consumes little power, and can be flush-mounted. The performance of the array, as well as that of the radiometer system in which it is used, has also been discussed.

Acknowledgment

Appreciation is extended to R. Bowers who assisted in the collection of a large portion of the data presented herein. Acknowledgment is also made of the efforts of the many others who have designed and assembled the overall radiometer system.

A Matrix-Fed Circular Array for Continuous Scanning

BORIS SHELEG

Abstract—**The Butler-matrix-fed circular array will form a focussed radiation pattern when the proper current distribution is established on the inputs to the matrix. Further, this beam can be scanned through 360° by changing only the phases of the matrix input currents, just as with a linear array scanning is accomplished by varying the phases of the element currents. This operation was experimentally demonstrated with a 32-dipole circular array and reasonable agreement was obtained between the measured and calculated patterns. Finally, a synthesis procedure is described for determining the matrix input currents required to attain a prescribed current distribution on the array.**

Manuscript received April 1, 1968; revised July 31, 1968.

The author is with the Microwave Antennas and Components Branch, Electronics Division, Naval Research Laboratory, Washington, D. C. 20390

Introduction

ANTENNAS consisting of radiating elements arrayed on a circle have been studied and have been used for many years, but recent developments in switching and phase shifting have led to a renewed interest in them. The appeal of the circular array is that, because of its

symmetry, it can be used to scan a beam in discrete steps through a full 360° without the variations in gain and pattern shape that occur when four linear arrays are used, each scanning through a single quadrant. The purpose of this study was to determine some of the possibilities and also the limitations of scanning with circular arrays and, in particular, to demonstrate the use of the Butler matrix in feeding the elements of the array. The idea of using a Butler matrix for this purpose is due to Shelton [1], who showed that it permitted the formation of a narrow radiated beam that could then be scanned essentially like the beam from a linear array, by the operation of phase shifters alone.

The operation of a Butler-matrix-fed circular array (multimode array) is first described heuristically in terms of "modes" and then, more satisfactorily, by considering the distribution of currents impressed on the radiating elements by the matrix. In addition, calculations were made to show how the radiation pattern of the multimode array varies as it is scanned continuously, rather than in discrete steps.

The experimental portion of this program was performed at L-band with a circular array of 32 dipoles around a conducting cylinder. Sidelobe level control was shown by using different amplitude tapers over the illuminated portion of the array.

Theory of Operation

The principles involved in scanning a multimode array are most easily seen by considering not an array, but a continuous distribution of current. When this distribution is expressed as a Fourier series, in general infinite, each term represents a current mode uniform in amplitude but having a phase varying linearly with angle. The radiation pattern of each mode has the same form as the current mode itself, and these pattern modes are the Fourier components of the radiation pattern of the original distribution. The expression of the radiation pattern as the sum of modes of this form is then seen to be analogous to the summation of the contribution made to the pattern of a linear array by its elements, so the operation of a multimode array can be explained by referring to an equivalent linear array.

Referring to Fig. 1, consider a current distribution $I(\alpha)$ to be the sum of a finite number of continuous current modes $I_n e^{jn\alpha}$ with $-N \leq n \leq N$. The radiation pattern for $\theta = \pi/2$, is then given by

$$E(\phi) = \sum_{n=-N}^{N} C_n e^{jn\phi} \tag{1}$$

where the C_n are complex constants given by

$$C_n = 2\pi K j^n I_n J_n\left(\frac{2\pi a}{\lambda}\right) \tag{2}$$

with K a constant [2]. There is a one-to-one correspondence between the current modes $e^{jn\alpha}$ and the far-field pattern modes $e^{jn\phi}$, but note that their relative phases are not necessarily the same. Another property peculiar to circular arrays with isotropic radiators is that some modes can be made to give zero contribution in the plane of the circle by the selection of a proper diameter. However, for practical

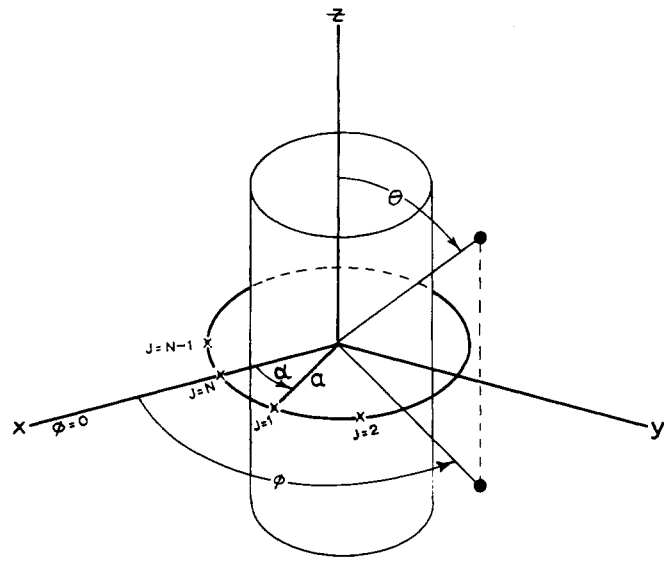

Fig. 1. Coordinates for a continuous cylindrical sheet of vertical current elements.

antennas of interest (e.g., dipoles approximately one-quarter wavelength over a reflecting cylinder) all the modes make contributions in the plane of the array.

Equations (1) and (2) demonstrate that a change in relative amplitude and phase of each current mode results in a corresponding change in the corresponding pattern mode (this can be done by controlling I_n). This is nearly identical to the formulation for linear arrays. A linear array of $2N+1$ isotropic elements with interelement spacing a has a radiation pattern given by

$$E(u) = \sum_{n=-N}^{N} A_n e^{jnu} \tag{3}$$

where $u = ka \sin \phi$, ϕ is the angle off-broadside, and A_n is the current on the nth element. Equations (1) and (3) show the similarity of the patterns of the circular current sheet and the linear array, with the role of the current mode in the circular array taken by the element in the linear array. One difference is that for the circular array the argument is ϕ, and for the linear array it is $ka \sin \phi$. A second difference is that equally excited elements in a linear array make contributions of equal magnitude to the radiation pattern, but equally excited current modes do not contribute equally, because their elevation patterns are not identical. This results in differences in their strength of contribution in the plane of the antenna. For example, if in the antenna being considered (Fig. 1) it is desired that the pattern modes be equal in magnitude and be in phase at $\phi = 0$, the excitations of the current modes must be [from (2)]

$$I_n = \frac{1}{2\pi K j^n J_n\left(\frac{2\pi a}{\lambda}\right)}. \tag{4}$$

Its radiation pattern is then given by

$$E(\phi) = \sum_{n=-N}^{N} e^{jn\phi}, \tag{5}$$

which may be summed to give the pattern characteristic of a uniform array

$$E(\phi) = \frac{\sin\left(\frac{2N+1}{2}\phi\right)}{\sin\frac{\phi}{2}}. \tag{6}$$

The beam can be scanned (in theory) by a linear variation of the phases of the mode excitations, just as the beam from a linear array is scanned by a linear variation of the element phases. If the phase difference between adjacent modes is ϕ_0 radians [multiplying I_n of (4) by $e^{-jn\phi_0}$], the resultant pattern is expressed as

$$E(\phi) = \frac{\sin\left[\frac{2N+1}{2}(\phi-\phi_0)\right]}{\sin\left(\frac{\phi-\phi_0}{2}\right)}, \tag{7}$$

which is the original pattern scanned ϕ_0 radians. Although the foregoing analysis was based on the particular example of a cylindrical sheet of infinitesimal current elements, the same reasoning applies to any circular antenna having similar pattern modes. The only difference in the analysis would be the particular relationship between the phases and amplitudes of the pattern modes and their respective current modes.

Various antennas have made use of the multimode principle in their operation [3]–[5] but, as has been mentioned, Shelton discovered that it was possible to excite simultaneously and independently all the modes, both positive and negative, from zero to $N/2$ by connecting a single ring of N elements to the outputs of a Butler matrix. That this is true is evident from the definition of the Butler matrix [6]. This matrix is a lossless, passive network having N inputs and N outputs, where N usually is some power of 2. The inputs are isolated from one another, and a signal into any input results in currents of equal amplitude on all the outputs with phase varying linearly across the elements. Specifically, if N is even and the Kth input port is energized ($K=0, \pm1, \pm2, \cdots, \pm(N-2)/2, N/2$), the difference in phase between adjacent ports is $2\pi K/N$ and the total phase variation around a circular array connected to the Butler matrix would be $2\pi K$, which is the Kth mode. Hence, with the Butler matrix we may establish on the array the N current modes corresponding to $K=0, \pm1, \cdots, \pm(N-2)/2, N/2$, and, because the input ports are isolated, the modes are independent. It should be noted here that there are Butler matrices that do not satisfy the definition given above and that cannot be used unmodified in a multimode array. These networks establish, across their outputs, linear phase progressions whose total variations are odd multiples of π radians. A matrix of this type can be changed to one having the proper modes by adding fixed phase shifts to all the output ports; if the N outputs are labeled $J=1, 2, \cdots, N$, the phase shift applied to the Jth output is $J\pi/N$.

A schematic diagram of a scanning multimode array is shown in Fig. 2. The desired phase and amplitude distribution is established over the inputs to the Butler matrix by fixed phase shifters and a corporate structure. Once the pencil beam pattern is formed at some azimuth angle, it is scanned just as in a linear array; the mode amplitudes are held fixed, and a linear phase progression is set up on the mode inputs by operating the variable phase shifters.

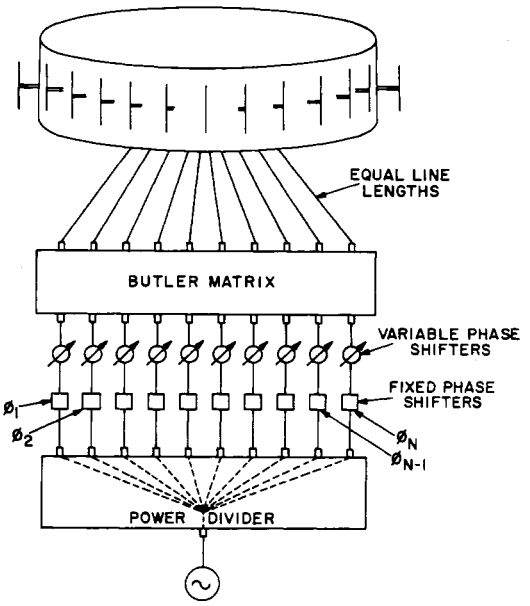

Fig. 2. Schematic diagram of a scanning multimode array.

Pattern Calculation

Thus far, the explanation of a multimode array has been based on the summation of pattern modes of the form $e^{jK\phi}$. The summation could be exactly achieved with a continuous current sheet, or it could be approximated arbitrarily well with a ring array having a sufficient number of elements. For arrays fed from a Butler matrix, as many current modes can be established as there are elements, and it is not obvious how many of these modes have far-field patterns that fit the $e^{jK\phi}$ form sufficiently well. For example, in an N-element array the highest order mode ($K=N/2$) has an element-to-element phase variation of π radians. By symmetry, its pattern must be scalloped, with N nulls and N peaks; therefore, it obviously cannot be used as a uniform mode.

To determine the quality of the modes established by the Butler matrix, a series of calculations was made, both of mode patterns and of pencil beam patterns obtained by summing different numbers of modes. The array consisted of 32 elements, and the interelement spacing was varied from 0.4 to 0.6λ. Two different element patterns were used, one was an approximation to the measured pattern of the elements that were actually used (dipoles around a cylinder) and the other was the exact pattern of an infinitesimal vertical current element in front of a conducting cylinder [7].[1]

[1] Also, for a more detailed description, see R. H. DuHamel, "Pattern synthesis for antenna arrays on circular, elliptical, and spherical surfaces," Elec. Engrg. Research Lab., University of Illinois, Urbana, Contract N6-ORI-71; Task 15, Tech. Rept. 16, May 1952.

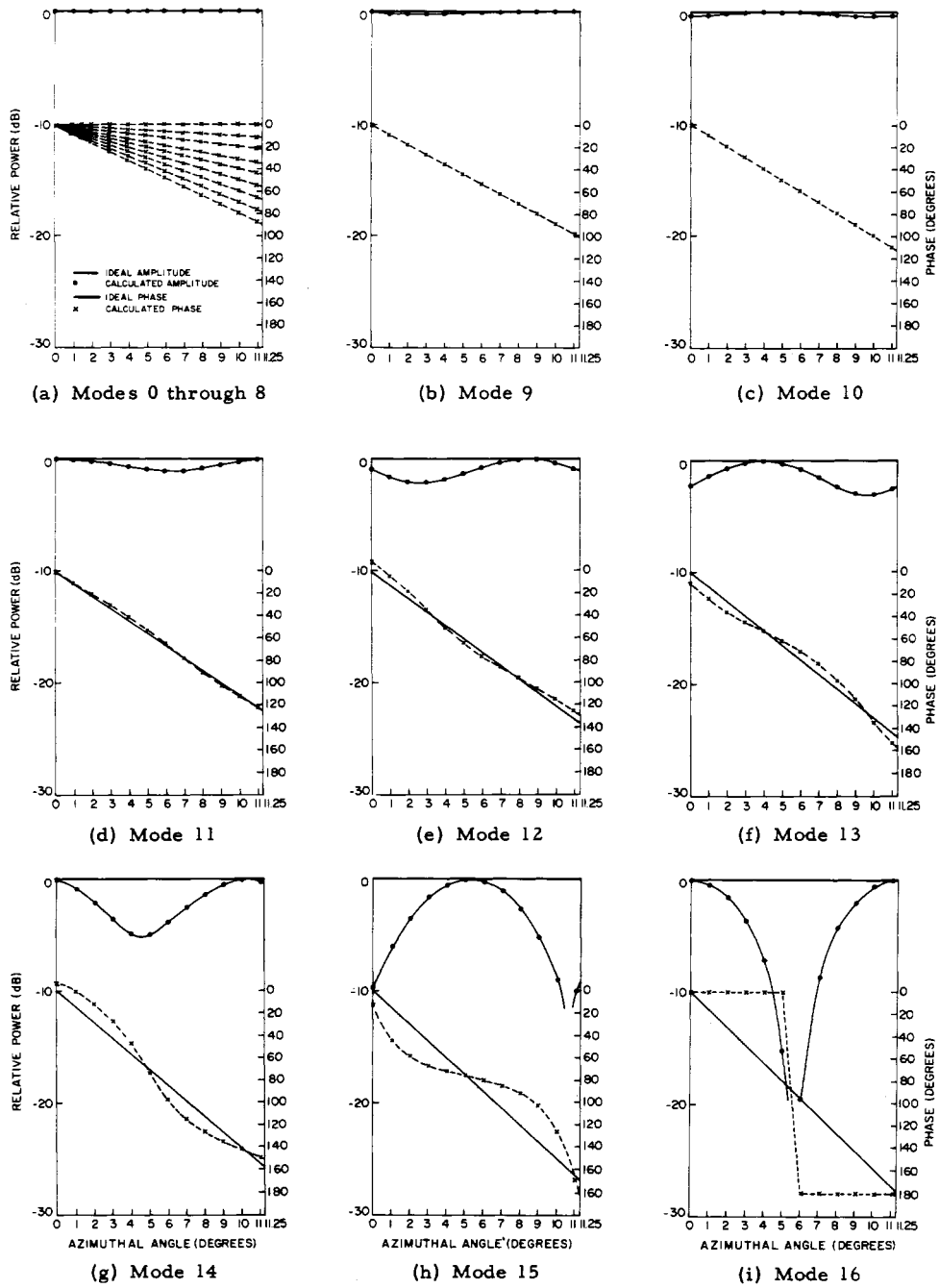

Fig. 3. Calculated mode patterns for a 32-dipole circular array compared with the ideal mode patterns.

The approximate pattern of the dipole in front of a cylinder is given by

$$A(\phi) = \tfrac{1}{2}(1 + \cos\phi), \tag{8}$$

where the phase was assumed constant in azimuth when referred to a point one-third the distance from the cylinder to the dipole. This assumption is reasonably good, at least in the unshadowed region. Mode patterns and pencil beam patterns computed using (8) were in good agreement with those obtained using the exact pattern of the vertical current element, and no results for the latter have been included.

Consider, as in Fig. 1, a circular array of radius R with N elements equally spaced at $\alpha_J = J2\pi/N$, where $J = 1, 2, \cdots, N$. Referred to the center of the circle, the relative space phase of the Jth element is $(2\pi R/\lambda)\cos(\phi - \alpha_J)$, where only the plane of the array is considered. If the element pattern is $A(\phi - \alpha_J)$ and the current on the element is $A_J e^{j\psi_J}$, the radiation pattern of the array is given by

$$E(\phi) = \sum_{J=1}^{N} A_J e^{j\psi_J} A(\phi - \alpha_J) e^{j(2\pi R/\lambda)\cos(\phi - \alpha_J)}. \tag{9}$$

Mode patterns were calculated from this equation with the element pattern given by (8) and, for the Kth mode, a current distribution given by $A_J = 1$, $\psi_J = 2\pi KJ/N$. Results are shown for a 32-element array, for which the modes correspond to $K = 0, \pm 1, \pm 2, \cdots, \pm 15, 16$. The phase and amplitude of computed mode patterns for a 32-element circular array (0.5λ spacing) are compared with ideal modes in Fig. 3. It is seen that all modes up to ± 10 are in sub-

TABLE I
THE RELATIVE GAINS AND PHASES OF THE PATTERN MODES OF A 32-ELEMENT ARRAY

Mode	Relative Gain (dB)	Relative Phase at $\phi=0$ (degrees)
0	0.0	0.00
1	0.2	0.74
2	0.1	7.51
3	0.2	14.63
4	0.2	29.27
5	0.0	44.63
6	0.5	63.06
7	0.2	91.93
8	−0.5	115.35
9	0.8	144.56
10	1.0	−168.45
11	−0.5	−128.07
12	0.7	−105.74
13	3.5	−35.18
14	5.1	20.91
15	5.6	120.92
16	5.6	−172.05

stantial agreement with the ideal patterns, having at most a ± 0.25-dB difference from a uniform pattern, with a maximum phase error of 3°. Modes ± 14, ± 15, and 16 are poor approximations. Mode patterns were also computed for arrays with element spacings of 0.4 and 0.6λ. With 0.4λ element spacing, modes up to ± 12 are close to ideal, and modes ± 15 deviate about as much as did modes ± 14 for the array with 0.5-λ spacing. For 0.6-λ spacing, modes up to ± 9 are good, and mode 12 corresponds to mode 14 for 0.5-λ spacing. Table I lists the relative gains of all the pattern modes for 0.5-λ spacing and also their relative phases at $\phi=0$ when the current modes are in phase at $\alpha=0$ (i.e., at element 32). To form a narrow beam with its peak at $\phi=0$, the pattern modes must be in phase in that direction; therefore, the phase differences between the modes must be accounted for, as shown in Fig. 2, by fixed phase shifts at the inputs to the Butler matrix.

The analysis of a circular array in terms of ideal modes is adequate for a qualitative description of its operation and does predict reasonably well the position and shape of the main lobe but not the structure of the sidelobes. For a more accurate estimate, the current distribution on the array must be determined, and the pattern must then be calculated from (9). First assume that the N-element Butler matrix has all the current modes in phase at the Nth element if the mode inputs are fed in phase; this means that for the Kth mode the Jth element has phase $2\pi KJ/N$. Then, if $B_K e^{j\beta_K}$ is the current applied to the Kth input port, the resultant $A_J e^{j\psi_J}$ on the Jth radiating element is given by

$$A_J e^{j\psi_J} = \frac{1}{\sqrt{N}} B_K e^{j\beta_K} e^{jKJ(2\pi/N)}. \tag{10}$$

If many input ports are simultaneously excited, the output currents may be added to give

$$A_J e^{j\psi_J} = \frac{1}{\sqrt{N}} \sum_K B_K e^{j\beta_K} e^{jKJ(2\pi/N)}. \tag{11}$$

This current distribution may then be substituted into (9) to give the radiation pattern expressed as

$$E(\phi) = \sum_{J=1}^{N} \left[\sum_K B_K e^{j\beta_K} e^{jJK(2\pi/N)}\right] \cdot A(\phi - \alpha_J) e^{j(2\pi R/\lambda)\cos(\phi-\alpha_J)}. \tag{12}$$

It is perhaps evident from the symmetry of the multimode array that the pattern shape does not change if the beam is scanned by some multiple of $2\pi/N$, the angle between elements. If for example, the beam is to be scanned $M(2\pi/N)$ radians, where M is an integer, the mode amplitudes B_K are held constant but there must be a mode-to-mode phase difference of $M(2\pi/N)$; hence, the phase of the Kth mode becomes $\beta_K + KM(2\pi/N)$. When this is substituted into (11), the current on the Jth radiating element is found to be

$$A_J e^{j\psi_J} = \frac{1}{\sqrt{N}} \sum_K B_K e^{j\beta_K} e^{j(M+J)K(2\pi/N)}, \tag{13}$$

showing that the original current distribution has been moved, intact, M elements around the array.

To show the formation of the radiation patterns as the modes are superimposed, patterns of a 32-element array with 0.5-λ spacing were computed from (12) using the cardioid element pattern of (8). With uniform excitation of the Butler-matrix inputs (all $B_K=1$) and with phases corresponding to those in Table I, the modes were successively excited and at each stage the radiation pattern was calculated, giving the series of patterns shown in Fig. 4. It can be seen that the beam narrows as more modes are added and that, until modes ± 11 are reached, the far-out sidelobes decrease as they would if the modes were perfect. This improvement ceases as the higher modes are added; when all the modes but the 16th are included, the pattern is noticeably worse than when just the modes up to ± 10 are used. The two patterns using modes up to ± 10 and up to ± 15 are compared in Fig. 5 with the patterns that would result if the corresponding numbers of ideal modes were summed. The agreement, when all the modes are used, is particularly poor in the region of the far-out lobes; when the less uniform modes (11)–(15) were not used, the patterns for the discrete and continuous cases agreed everywhere to within 0.5 dB. It is interesting to note that about 95 percent of the total power is radiated by the 13 elements nearest the direction of the beam and that the currents on 11 of these differed in phase from the cophasal condition by less than 20°.

The sidelobes from a linear array can be lowered by tapering the amplitude distribution over the array, and, by analogy, the same should be true for a circular array if the mode amplitude distribution is tapered. With the phases again as in Table I, a cosine taper was applied to the mode inputs [i.e., $B_K=\cos(K\pi/32)$], and the patterns were computed as modes were added successively. Fig. 6 is a comparison of the final pattern, when all the modes were used, with the pattern that would result if the modes were ideal. This shows that the sidelobe level has indeed been reduced but not to the level that would be obtained with perfect modes. In this

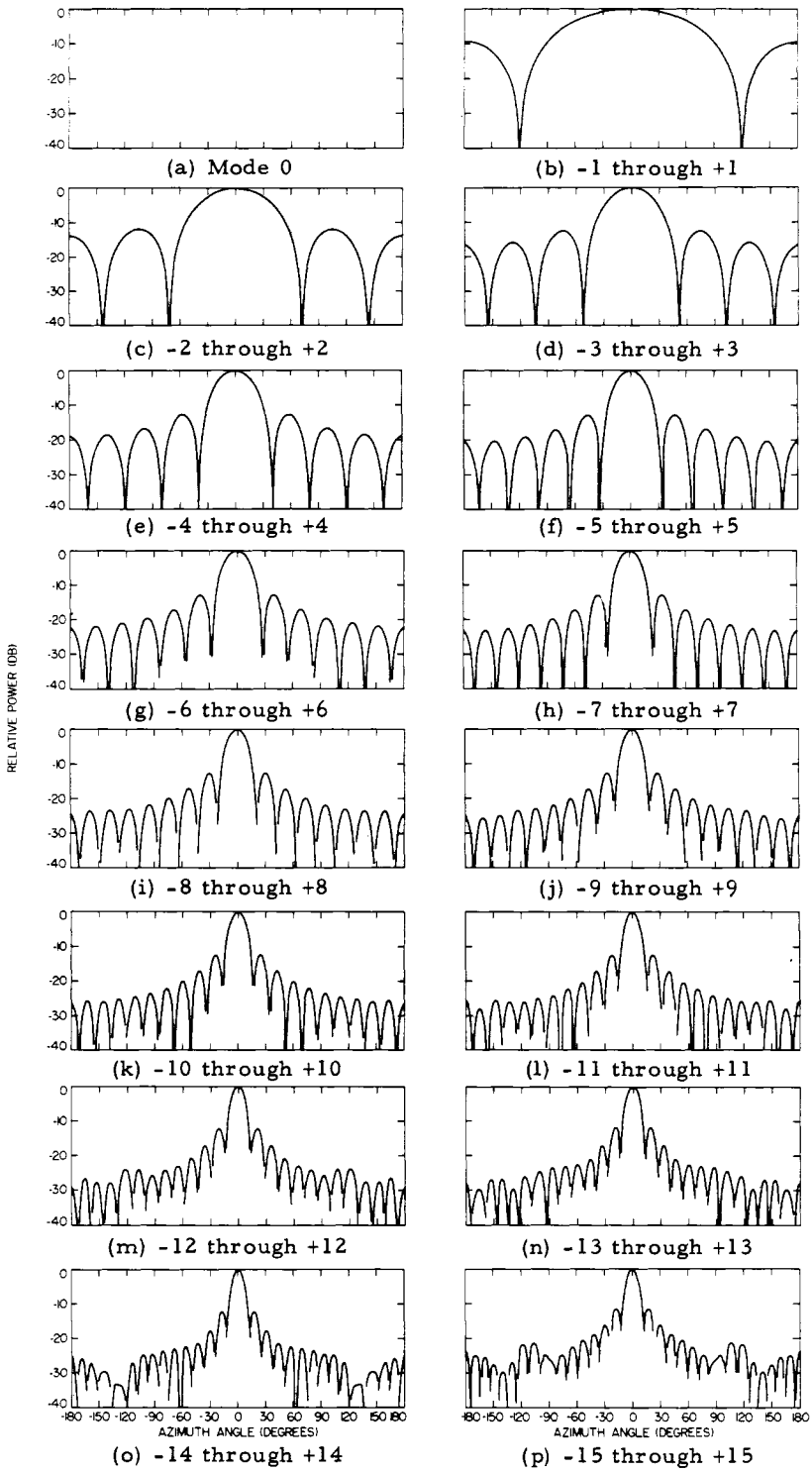

Fig. 4. Mode-by-mode buildup of the pattern of a 32-element array with uniform excitation of the modes.

case more than 95 percent of the total power is radiated from the 9 elements closest to the beam and on these elements the currents differ from cophasal by at most 5°.

One of the distributions used in the experimental program was $B_K = \cos^2(\pi K/40)$, which provided a 17-dB taper over the 31-mode inputs. To indicate how much the pattern shape could be expected to change as the beam was scanned, patterns were computed for various beam positions. Fig. 7 shows three patterns, one phased so that its peak is in the direction of element 32 ($\phi = 0$), the other two having the same amplitude distribution over the modes but phased to scan the beam one quarter and one half, respectively, of the angle between elements. It may be seen that, at least for this distribution, the pattern changes only slightly as the beam is scanned.

Patterns were also calculated for different element spacings, element patterns, and amplitude distributions, but those shown satisfactorily illustrate the beam formation

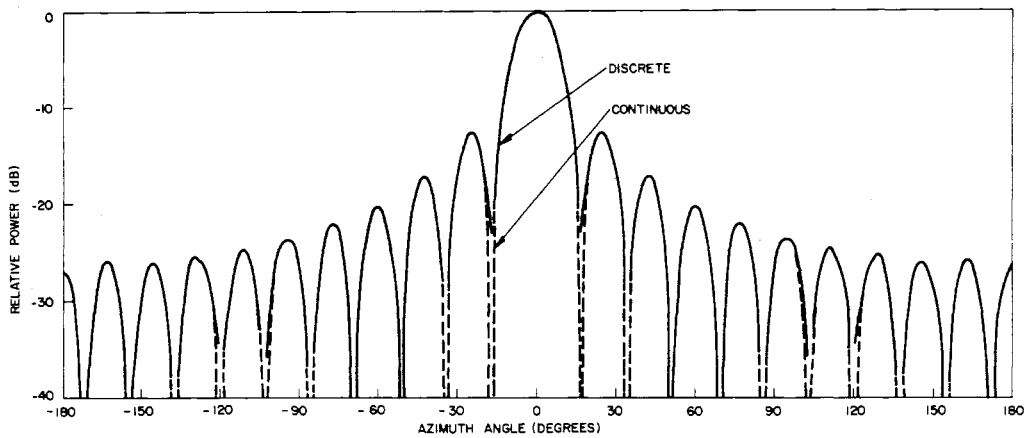

(a) Sum of modes -10 through +10

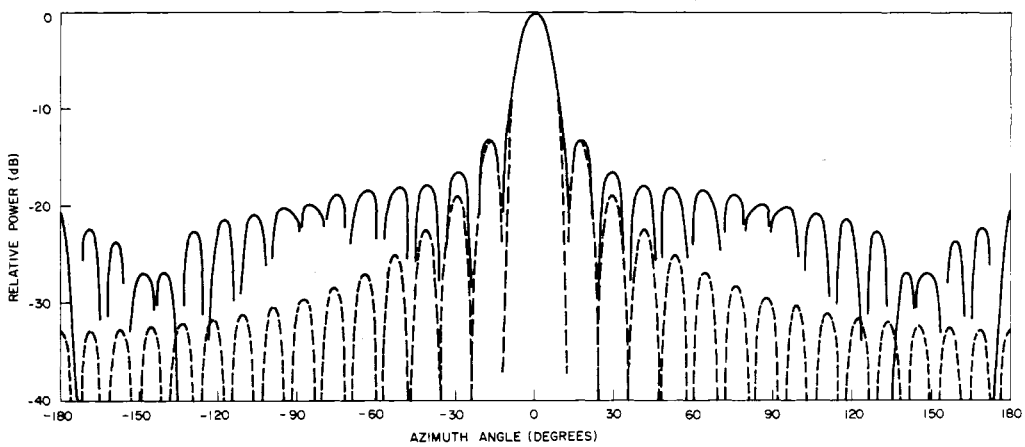

(b) Sum of modes -15 through +15

Fig. 5. Comparison of the patterns of a 32-element array and of a continuous current sheet using 21 and then 31 uniformly excited modes.

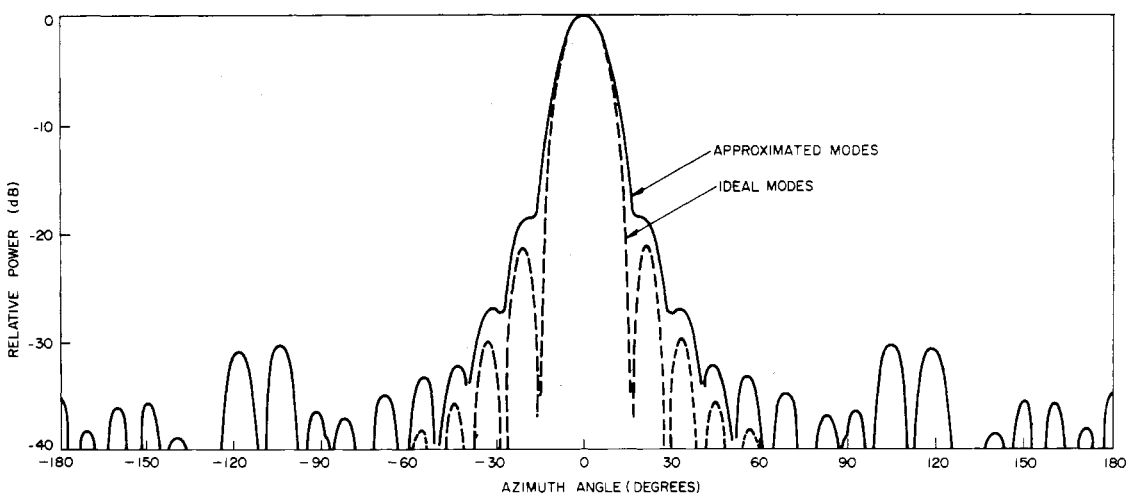

Fig. 6. Comparison of the patterns of a 32-element array and of a continuous current sheet using cosine amplitude taper on 31 modes.

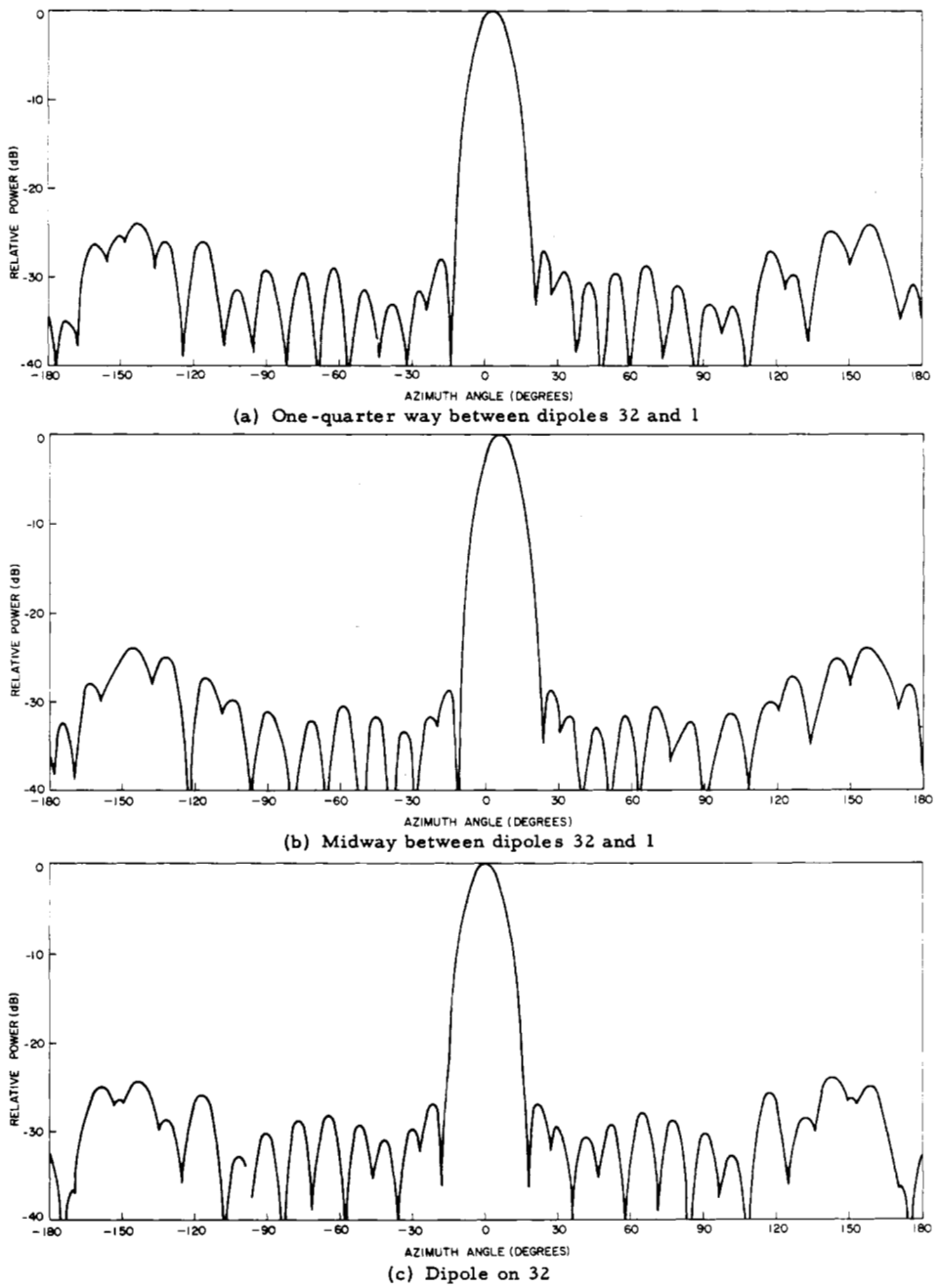

Fig. 7. Patterns and the corresponding current distributions on a 32-element array for beams at 0°, 5.625°, and 2.813°. The amplitude taper on the modes is $B_K = \cos^2(\pi K/40)$ with $K = 0, +1, \pm 2, \cdots, \pm 15$.

and scanning and also indicate how the pattern differs from one based on the existence of perfect pattern modes.

Synthesis of Aperture Distributions

It should now be evident that the radiation pattern of a circular array computed on the assumption that the pattern modes are perfect is not the same as that computed from the actual current distribution, and that a certain amount of cut-and-try is involved in determining the number of modes to use and in adjusting the phases of the modes to form a beam in a particular direction. Instead of picking the mode excitations, only to find that the corresponding current distribution results in a poor radiation pattern, it would be preferable first to pick a current distribution having an acceptable pattern and then to find the mode excitations which will give these currents. That this is always possible was discovered by Davies [8], who showed that any prescribed output currents can be achieved with a Butler matrix by properly exciting the matrix inputs.

Consider an $N \times N$ Butler matrix with input and output ports labeled K and J, respectively. If the prescribed currents $A_J e^{j\psi_J}$, where $J = 1, 2, \cdots, N$ are to be set up on the array, the N currents that must be applied to the inputs of the matrix are

TABLE II
COPHASAL DISTRIBUTION FOR THE BEAM AT 5.625° WITH REQUIRED INPUT CURRENTS AND THE CURRENT DISTRIBUTION ON THE ARRAY FOR BEAMS SCANNED TO 8.438° AND 11.25°

Input to Modes			Beam Position											
			Between Elements 32 and 1				On Element 1				One-Quarter Way Between Elements 1 and 32			
Mode	Amplitude	Phase (rad)	Element	dB	Phase	Cophasal Deviations	Element	dB	Phase	Cophasal Deviations	Element	dB	Phase	Cophasal Deviations
−15	0.05014	−2.98853	1	0.00000	4.41432	0.0	1	0.00000	1.30606	1.3	1	0.00000	1.98974	0.1
−14	0.16982	−2.80781	2	−0.51926	39.47402	0.0	2	−2.01691	17.80973	0.2	2	−1.64249	28.35642	0.6
−13	0.31358	−2.60148	3	−1.43457	108.24662	0.0	3	−1.10324	64.83482	5.0	3	−1.45862	83.40640	5.6
−12	0.43767	−2.37450	4	−2.84185	−151.91152	0.0	4	−2.07344	160.91891	6.4	4	−2.17622	−176.63541	0.1
−11	0.51999	−2.09735	5	−4.93675	−24.83651	0.0	5	−5.79880	−80.13033	11.4	5	−5.09892	−48.91991	8.0
−10	0.59752	−1.76797	6	−8.17489	124.58780	0.0	6	−10.95202	43.41646	3.0	6	−10.31497	94.83752	5.0
−9	0.68904	−1.42198	7	−14.02687	−69.38130	0.0	7	−13.44224	164.97679	10.9	7	−18.95701	−132.54333	26.00
−8	0.73786	−1.03866	8	−110.95878	9.40060	—	8	−13.49060	−44.26421	62.2	8	−18.54252	−39.69405	—
−7	0.70416	−0.53875	9	−110.29151	−127.37128	—	9	−19.78507	147.62327	—	9	−23.49840	149.10857	—
−6	0.63277	0.07777	10	−108.42737	−80.12002	—	10	−22.97828	−27.73955	—	10	−26.36628	−26.97267	—
−5	0.49759	0.68746	11	−112.01176	103.52423	—	11	−25.16028	154.81247	—	11	−28.37765	155.27371	—
−4	0.23592	1.46408	12	−111.17657	−75.03709	—	12	−26.75804	−23.60801	—	12	−29.86092	−23.31109	—
−3	0.17912	−2.74105	13	−107.88319	−119.27306	—	13	−27.94438	157.42682	—	13	−30.96016	157.62730	—
−2	0.25706	−1.78156	14	−117.77163	34.95047	—	14	−28.80676	−21.90153	—	14	−31.75041	−21.77114	—
−1	0.25264	−0.54328	15	−112.87704	65.89978	—	15	−29.39541	158.52920	—	15	−32.27577	158.60405	—
0	0.41310	0.25664	16	−117.61885	−131.95122	—	16	−29.73847	−21.22499	—	16	−32.56037	−21.19276	—
1	0.41310	0.35481	17	−118.16084	−136.67705	—	17	−29.85107	158.85470	—	17	−32.61636	158.85068	—
2	0.25264	−0.24785	18	−111.86473	60.67050	—	18	−29.73843	−21.22460	—	18	−32.44693	−21.26605	—
3	0.25706	−1.29069	19	−122.53436	43.74770	—	19	−29.39536	158.52921	—	19	−32.04448	158.44071	—
4	0.17912	−2.05383	20	−107.81624	−112.96098	—	20	−28.80673	−21.90223	—	20	−31.39070	−22.04947	—
5	0.23592	2.34765	21	−114.45265	−75.31601	—	21	−27.94435	157.42611	—	21	−30.45327	157.20708	—
6	0.49759	1.76738	22	−116.41499	94.23270	—	22	−26.75802	−23.60789	—	22	−29.17439	−23.93888	—
7	0.63277	1.35404	23	−109.30689	−95.61509	—	23	−25.16029	154.81323	—	23	−27.45203	154.29411	—
8	0.70416	0.93386	24	−113.19501	−108.60654	—	24	−22.97834	−28.73904	—	24	−25.07565	−28.62743	—
9	0.73786	0.63030	25	−113.92446	8.94868	—	25	−19.78514	147.62316	—	25	−21.47069	145.78916	—
10	0.68904	0.44333	26	−14.02684	−69.38122	0.0	26	−13.49063	−44.26440	62.2	26	−12.17991	−51.94113	—
11	0.59752	0.29369	27	−8.17489	124.58789	0.0	27	−13.44226	164.97683	10.9	27	−9.45066	143.16679	28.0
12	0.51999	0.16066	28	−4.93675	−24.83631	0.0	28	−10.95202	43.41665	3.0	28	−7.73339	1.07559	13.00
13	0.43767	0.07986	29	−2.84186	−151.91129	0.0	29	−5.79880	−80.13017	11.4	29	−5.12229	−118.84582	0.2
14	0.31358	0.04923	30	−1.43458	108.24684	0.0	30	−2.07344	160.91905	6.4	30	−2.07351	135.92040	5.0
15	0.16982	0.03925	31	−0.51925	39.47413	0.0	31	−1.10324	64.83485	5.0	31	−0.76244	51.05834	4.0
16	0.05014	0.05488	32	−0.00002	4.41439	0.0	32	−2.01692	17.80984	0.2	32	−1.35198	9.49976	3.5

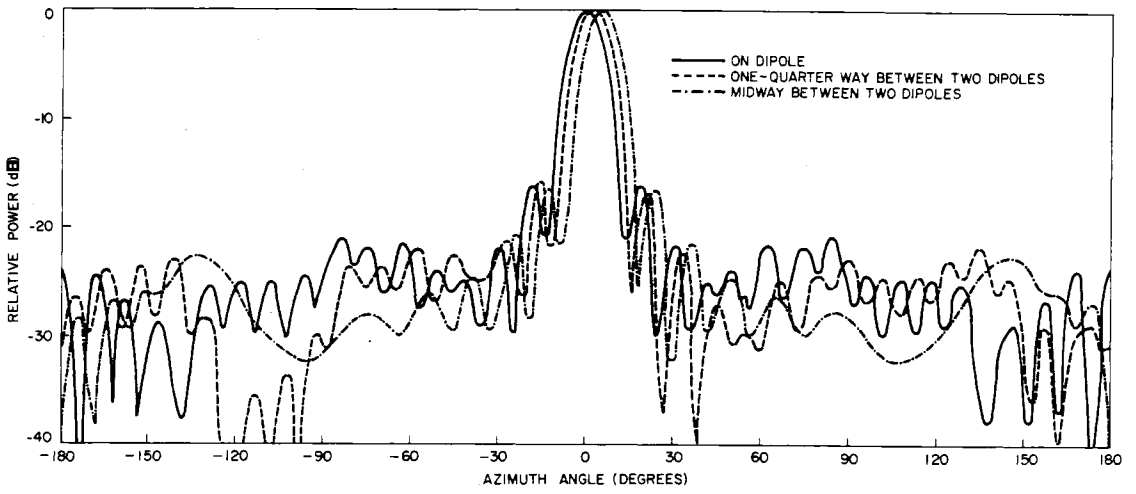

Fig. 8. Pattern of the 32-element array with a synthesized cophasal distribution and the pattterns when scanned to 8.44° and 11.25°.

$$B_K e^{j\beta_K} = \sum_{J=1}^{N} A_J e^{j\psi_J} e^{-jKJ(2\pi/N)}. \tag{14}$$

These currents are conjugate to those that would appear at the inputs if currents $A_J e^{-j\psi_J}$ were fed into the outputs of the matrix. The correctness of (14) may be verified by substitution into (11). As has been shown previously, since the matrix has a zero mode (looking from input to output), the current distribution that has been set up can be moved, intact, M elements around the array by holding the amplitudes B_K of the input currents fixed but changing their phases by applying a linear phase progression with a mode-to-mode phase difference of $M(2\pi/N)$.

It has been shown that the current distribution and the radiation pattern of a multimode array are invariant (aside from rotation) if the beam is scanned in steps equal to the angle between elements. For any other angle of scan, the current distribution will be changed. If, for example, all inputs are fed in phase with equal amplitude, only element N will be excited. If the linear phase progression $e^{-jK(2\pi/N)}$

is then applied to the inputs, the excitation is switched to element 1. If, however, the linear phase progression were only half this (i.e., $e^{-jK\pi/N}$), two elements, N and 1, would be strongly excited, but there would be currents on all the elements of the array. As a practical example, consider a 32-element array with a cophasal distribution on the 14-element sector which includes elements 26–7. The desired amplitude distribution is cos $[(K-1/2)\pi/16]$, which is symmetrical about a point midway between elements 32 and 1, and the elements are to be phased to form a beam in this direction. All other elements are to be inert. To show how the current distribution varies as the beam is scanned in small steps, the input currents required to achieve this distribution are first determined from (14), then their phases are changed to scan the pattern and the new distribution on the array is computed from (11). Table II gives the original distribution, phased for a peak at $\phi=5.625°$, and the corresponding input currents to the Butler matrix. Also in Table II is the distribution on the array when the beam is scanned to 11.25° (the direction of element 1) and the distribution when the beam is scanned to the angle midway between the first two. It is seen that, for the scanned beams, the currents are no longer confined to a sector; all elements are illuminated, with those on the rear of the array about 30 dB down. The stronger currents are on 15 or 16 elements, and over this sector there are only minor amplitude ripples with the currents differing from the cophasal condition by about 20°. The two scanned patterns (Fig. 8) do not differ significantly from the original one. Their beamwidths, near-in sidelobes, and the general level of their far-out lobes are comparable. If this distribution had been designed for very low sidelobes, it is likely that the pattern changes would have been more significant.

Experimental Program

The circular array used in the experimental program had 32 elements and was operated at 900 MHz. Various radiating elements were used: dipoles, short back-fire elements, and Yagis (the latter two to reduce the elevation beamwidth without increasing the height of the antenna), but the only array that will be described is a 32-element array of slot-fed dipoles, vertically polarized, spaced 0.5λ apart and 0.25λ from a conducting cylinder. This antenna is shown in Fig. 9 and the associated beamforming and scanning network is shown in Fig. 10. Since 3-dB quadrature couplers were used in the matrix, it had no zero mode; therefore, the coaxial cables connecting the matrix to the dipoles had to be cut to the proper lengths to correct for this. Corporate structures made in triplate line were used to establish the various amplitude distributions over the inputs to the Butler matrix.

The measured mode patterns for this array (Fig. 11) do not compare favorably with the computed patterns in Fig. 3. The deviations are attributable primarily to phase and amplitude errors in the matrix. All the current modes were fed so as to have the same phase at element 32, and the relative phases of the pattern modes were determined by comparing

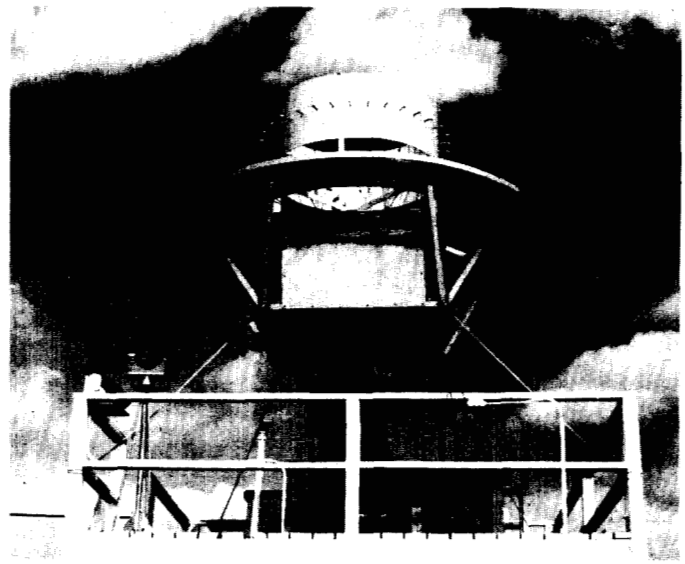

Fig. 9. Circular array of 32 dipoles ($\lambda/2$ spacing, 900 MHz).

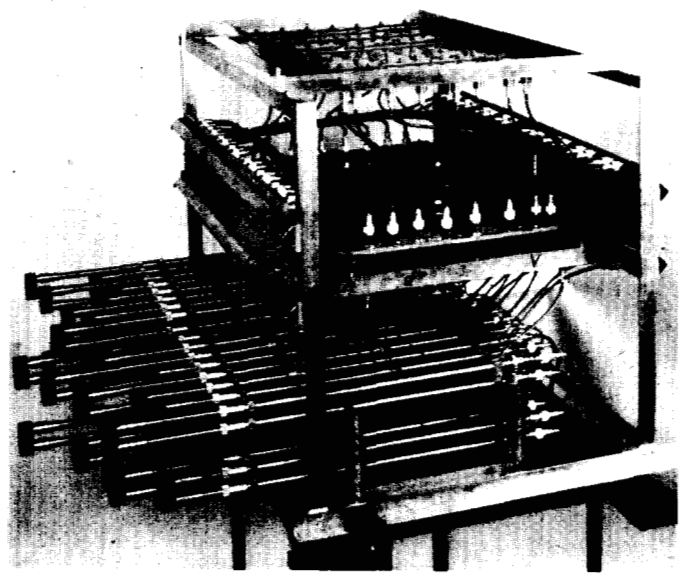

Fig. 10. Beam-forming and scanning network for the 32-dipole array.

the phase of each mode with that of the zero mode in the far field at $\phi=0$.

Fig. 12 shows the pattern of the array when a corporate structure was used providing currents of equal amplitude to all the mode inputs but number 16. For comparison, the corresponding calculated pattern (from Fig. 5) is shown solid. The two patterns agree reasonably well; both have beamwidths of about 10°, the measured first sidelobes are 1.5 dB higher than those calculated, and the general level of the far-out sidelobes is about 21 dB down for both.

The next series of patterns was taken with a tapered amplitude distribution over the modes. By dividing the outputs with tees, 31 modes were fed from a 16-element corporate structure. This resulted in a stepped distribution (since pairs of adjacent modes had equal amplitudes) with a 17-dB taper. The measured beamwidth (11.5°) and the first side-

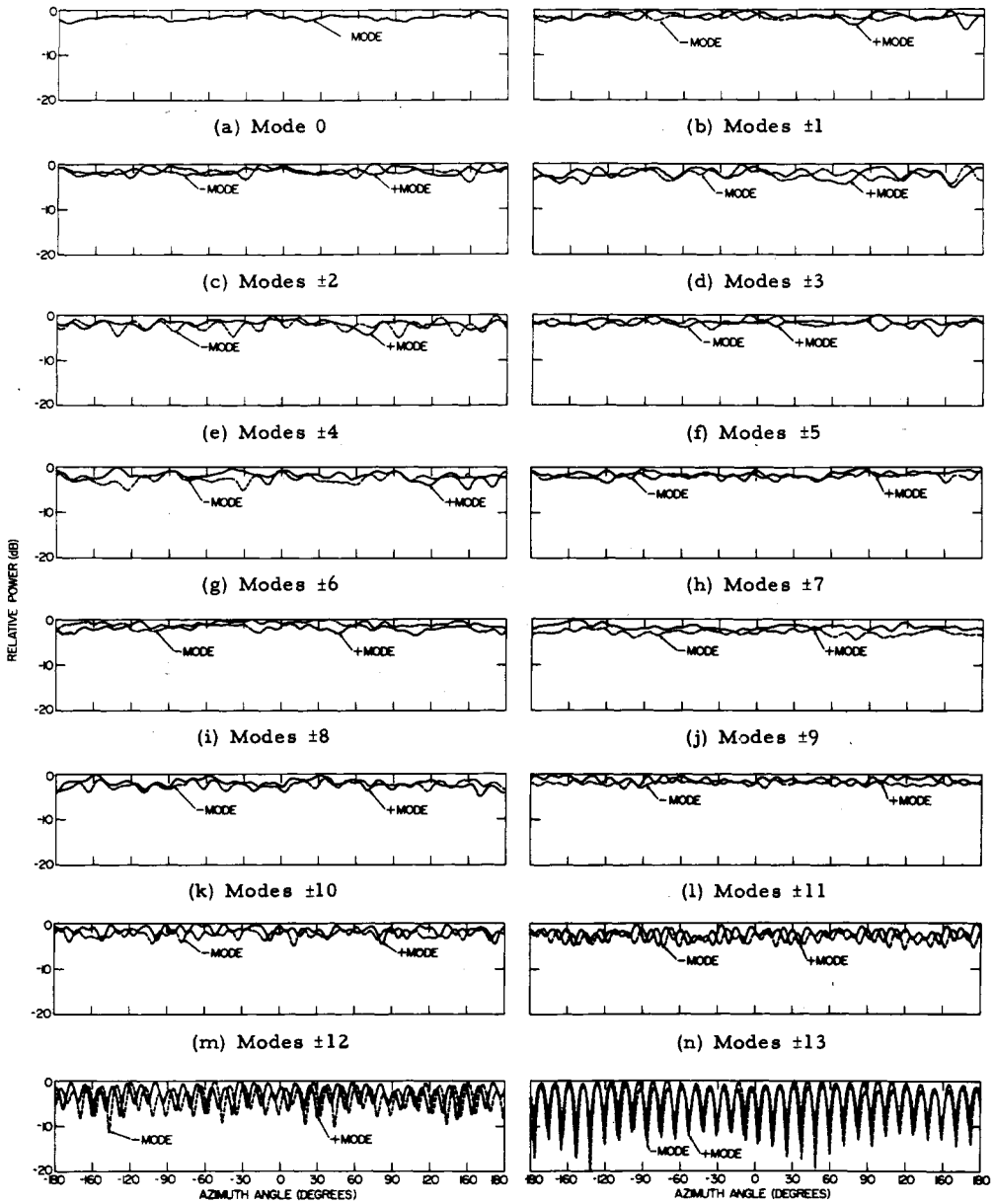

Fig. 11. Measured mode patterns for the 32-dipole array.

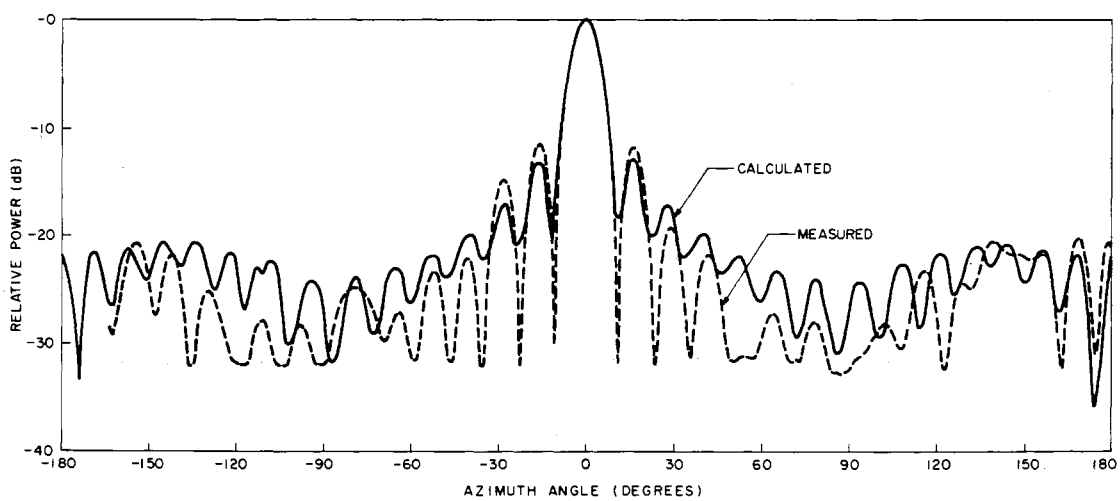

Fig. 12. Measured and calculated patterns of the 32-element array with uniformly excited modes.

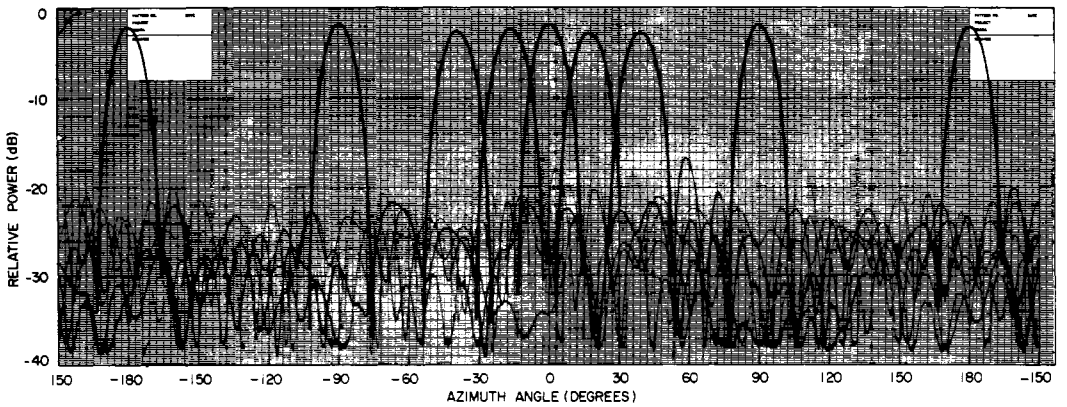

Fig. 13. Scanned patterns for the 32-element array with a tapered stepped distribution on the modes.

lobe (19 dB down) agree well with those calculated, but the level of the far-out lobes was somewhat worse than for the calculated pattern. The beam was then scanned by operating the phase shifters, and some of the patterns are shown in Fig. 13. It was found that the beamwidth and sidelobe level changed only slightly, and the gain varied by about 1 dB as the beam was scanned.

Conclusions

It has been shown that a Butler matrix can be used to feed a circular array to form a narrow pattern that can be scanned through 360° in azimuth by the operation of phase shifters alone. One explanation of this, based on the assumption that the radiation pattern could be written as the sum of a finite number of uniform pattern modes, was found to work only qualitatively in that it could not be used to predict the structure of the sidelobes. A 32-element array of dipoles was used to demonstrate experimentally how a beam was formed by superposition of the pattern modes (even though imperfect) and how the scanning was performed. Finally, the synthesis procedure of Davies was described, and as an example, the inputs to the Butler matrix required to achieve a prescribed cophasal sector distribution on the array were determined and the change in the current distribution for other beam positions were shown.

Acknowledgment

The author acknowledges the help given by R. M. Brown through numerous discussions and consultations, the contributions of F. W. Lashway, who was responsible for the mechanical design, and of R. J. Wiegand, who helped with the measurement program. In addition, the author expresses his gratitude to J. Tyszkiewicz of the Naval Air Systems Command, who sponsored and supported this work.

References

[1] G. C. Chadwick and J. C. Glass, "Investigation of a multiple beam scanning circular array," Scientific Rept. 1 to USAF Cambridge Research Lab., Cambridge, Mass., Contract AF19(628)367, December 31, 1962.

[2] W. R. LePage, C. S. Roys, and S. Seely, "Radiation from circular current sheets," *Proc. IRE*, vol. 38, pp. 1069–1072, September 1950.

[3] R. C. Honey and E. M. T. Jones, "A versatile multiport biconical antenna," *Proc. IRE*, vol. 45, pp. 1374–1383, October 1957.

[4] A. C. Schell and E. L. Bouché, "A concentric loop array," *IRE WESCON Conv. Rec.*, vol. 2, pt. 1, pp. 212–215, August 1958.

[5] C. P. Clasen, J. B. Rankin, and O. M. Woodward, Jr., "A radial-waveguide antenna and multiple amplifier system for electronic scanning," *RCA Rev.*, vol. 22, no. 3, pp. 543–554, 1961.

[6] J. L. Butler, "Digital, matrix, and intermediate-frequency scanning," in *Microwave Scanning Antennas*, vol. 3, R. C. Hansen, Ed. New York: Academic Press, 1966, ch. 3.

[7] P. S. Carter, "Antenna arrays around cylinders," *Proc. IRE*, vol. 31, pp. 671–693, December 1943.

[8] D. E. N. Davies, "A transformation between the phasing techniques required for linear and circular aerial arrays," *Proc. IEE* (London), vol. 112, pp. 2041–2045, November 1965.

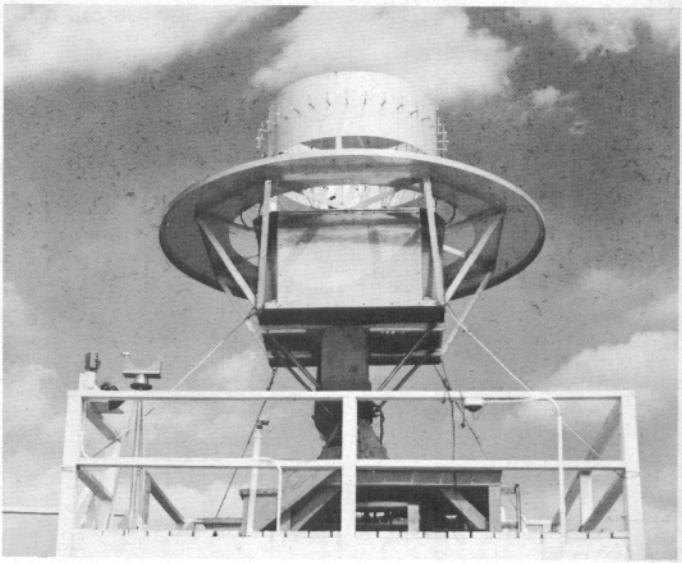

Fig. 9. Circular array of 32 dipoles ($\lambda/2$ spacing, 900 MHz).

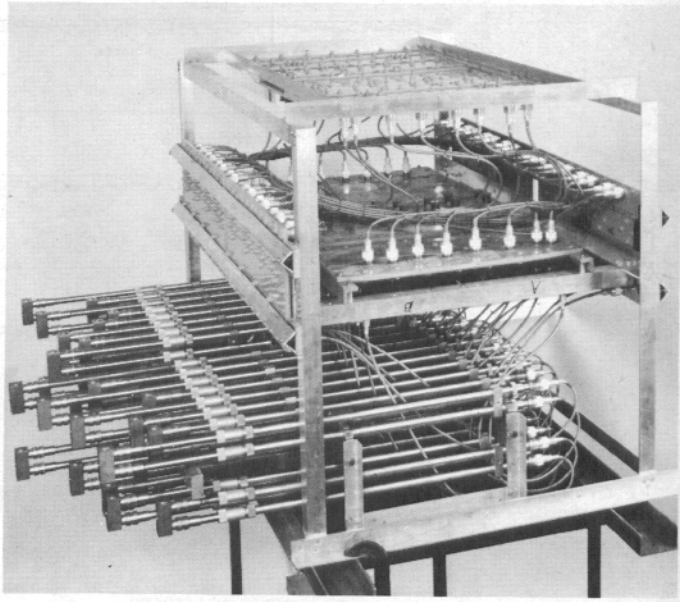

Fig. 10. Beam-forming and scanning network for the 32-dipole array.